Research on Engineering Structures & Materials
www.jresm.org
MIM Research Group

Research Article

Comparative analysis of R/SWIR, NIR/SWIR, and NDSI classification methods for determination of snow cover change on Erciyes Mountain, Türkiye using Landsat satellite images

Mustafa Hayri Kesikoglu*,1,2,a

[1]*Dept. of Civil Eng., Faculty of Engineering and Natural Sciences, Uşak University, Uşak, Türkiye*
[2]*Dept. of Urban and Regional Planning, Faculty of Architecture and Design, Uşak University, Uşak, Türkiye*

Article Info

Article History:

Received 10 Nov 2024

Accepted 11 Jan 2025

Keywords:

Change detection;
Classification;
Near-infrared/shortwave-infrared;
Normalized difference snow index;
Red/shortwave-infrared;
Remote sensing;
Snow cover

Abstract

Snow is a crucial factor impacting many areas, including freshwater resources, irrigation, floods, and avalanches. The study aims to compare the performances of unsupervised classification methods namely Normalized Difference Snow Index (NDSI), Red/Shortwave- infrared (R/SWIR), and Near-infrared/Shortwave-infrared (NIR/SWIR) band ratio methods in snow cover classification while determining the temporal change and trend in snow cover area during the past three decades on Erciyes Mountain. The study analyzed the snow cover on Erciyes Mountain from 1988 to 2020 using Landsat 5 TM and Landsat 8 OLI data with a spatial resolution of 30 meters. Three unsupervised classification methods were applied to atmospheric-corrected Landsat datasets to obtain snow cover maps. The results indicate a declining trend in snow cover on Erciyes Mountain due to global warming, with a significant reduction of about 87% over the past 32 years. Among the three classification methods, NDSI demonstrated the highest accuracy and Kappa coefficient, making it the most suitable approach for snow cover mapping in mountainous regions. The findings can supply valuable contributions to literature and assist in better use of accurate snow cover classification methods in high mountainous regions.

1. Introduction

Snow is an important factor of the global water cycle [1]. As a significant precipitation type, it provides approximately one-sixth of the global population's water needs [2]. Its ability to store water in winter and release it in summer contributes to the regulation of water resources management and ecosystem health. Moreover, snow cover significantly influences local and regional climates, making its accurate monitoring essential for water management and climate modeling [3-5].

However, due to global warming and other climate change impacts, snow-cover areas are undergoing significant changes. These changes directly affect the seasonal distribution of water resources, hydrological cycles, and ecosystems, leading to issues such as water scarcity, flood risks, and biodiversity loss. Therefore, monitoring changes in snow cover areas and understanding the impacts of these changes is of paramount importance for sustainable water resource management and climate change adaptation efforts.

Given the rapidly increasing population and the impacts of global warming, snow cover monitoring and data extraction have become even more critical. Studies on snow cover

*Corresponding author: hayri.kesikoglu@usak.edu.tr; mkesikoglu@gmail.com
[a]orcid.org/0000-0001-5199-0815
DOI: http://dx.doi.org/10.17515/resm2025-524ml1110rs

areas can provide valuable insights into the global water and energy cycle, aiding in its better understanding and management.

Ground-based classical measurement methods can be used for snow cover monitoring, but these methods have some limitations. Therefore, measurements using remote sensing data offer an important alternative for fast and effective monitoring of large areas [6-8]. Remote sensing has become a critical tool for monitoring snow cover changes with the ability to make synchronous observations over large areas [4, 9]. Xi and Mei [10] note that remote sensing technology has become a fundamental approach for large-scale and high-precision snow monitoring, reinforcing the statement about the critical role of remote sensing in observing snow cover changes. Largeron, Dumont [11] emphasized that remote sensing is essential for detecting snow cover changes that cannot be effectively monitored through point measurements alone. Girotto, Musselman [12] highlighted the extensive coverage provided by remote sensing images, allowing for reliable seasonal snow monitoring in remote and complex mountainous regions. In addition, remote sensing data have the potential to overcome the limitations of terrestrial measurements by providing high resolution and consistency to monitor snow cover changes over large areas [9, 13]. Therefore, remote sensing stands out as an indispensable tool for snow cover monitoring and management.

Index and band ratio-based unsupervised classification methods for snow cover classification are used in remote sensing data analysis. These methods use combinations of various spectral bands to map snow cover accurately. Various index and band ratio-based unsupervised classification methods to determine snow cover using remote sensing images have been employed in some studies. Ambinakudige, Inamdar [14] analyze how NIR and SWIR band's spectral characteristics can be utilized to improve the accuracy of snow cover mapping, reinforcing the importance of using band ratios in remote sensing applications. Butt [15] calculated three band ratios (Band 2/Band 5, Band 4/Band 5, and Band 4/Band 7) using Landsat data for snow zoning mapping in the Hindukush, Karakoram, and Himalayan regions. He stated that the band ratios effectively minimized the shadow effect. Wang, Wang [16] proposed a spectral band ratio using near-infrared (NIR) and short-wave infrared (SWIR) bands to map snow cover in dense coniferous forests using Landsat 8 Operational Satellite Imager (OLI) data. Zhang, Wang [17] introduced a new index that optimizes the use of R/SWIR and NIR/SWIR band ratios to improve the mapping accuracy of debris-free glaciers. The authors compare the performance of these band ratios against traditional methods, demonstrating their effectiveness in reducing classification errors related to water and shadow. Andreadis and Lettenmaier [18] used a snow mapping algorithm based on two indices, namely the normalized difference vegetation index (NDVI) and NDSI, to integrate remotely sensed snow observations into a macroscale hydrology model. Sibandze, Mhangara [19] aimed to increase the snow cover mapping accuracy by combining Principal Component Analysis (PCA) with NDSI by proposing the Normalized Difference Principal Component Snow Index (NDPCSI) technique. They showed that the use of PCA along with NDSI can increase the accuracy of snow cover mapping. Kuter, Akyürek [20] used NDSI to create a conventional binary reference snow map that classifies the MODIS satellite image as snow or non-snow. This study highlights the importance of NDSI in snow cover classification. Similarly, Liu, Huang [21] used machine learning technologies and NDSI methods to map snow cover fractions using MODIS data. The study demonstrates the effectiveness of NDSI in snow cover classification. However, these methods also have some disadvantages. Such index and band ratio-based studies can sometimes make it difficult to classify mixed pixels correctly and affect the accuracy and precision in snow cover classification [22]. While these studies show that index and band ratio-based methods are used in snow cover

classification, they also highlight some limitations of these methods. Therefore, considering these disadvantages, this study investigates which of the R/SWIR, NIR/SWIR, and NDSI methods used for snow cover classification gives better results in snow cover classification at Erciyes Mountain.

Previous research has primarily concentrated on glacial changes at Erciyes Mountain [23-25]. It was stated that the glaciers melted over time and almost disappeared [25]. However, the change in the amount of snow cover was not examined. This study has two main aims. The first aim of the study is to determine the temporal change and trend in snow-cover areas. The study analyzes the temporal change and trend in snow cover on Erciyes Mountain, covering 32 years from 1988 to 2020, using 30-m spatial resolution Landsat 5 TM and Landsat 8 OLI data. While a large part of Erciyes Mountain is completely covered with snow in the winter season, a portion of this area is covered with snow in the summer months as well. Satellite images from the summer months were preferred to minimize the impact of high cloud cover at the summit. The second aim of the study is to compare the performance of unsupervised classification methods in snow cover classification. R/SWIR, NIR/SWIR, and NDSI methods were applied to the atmospherically corrected Landsat data sets to obtain snow cover maps. As a result of the assessments, the best unsupervised classification technique for snow-covered mountains similar to the Erciyes was determined.

2. Materials

2.1. Study area and data

Erciyes Mountain is a volcanic mountain located in Kayseri Province, Turkey, with an elevation of 3,917 meters [26]. This region provides an important natural area for studying snow cover dynamics. Erciyes Mountain significantly impacts water resources due to the heavy snowfall during the winter months and the melting of this snow cover during the summer months.

Landsat 4–5	Bands	Wavelength (micrometers)	Resolution (meters)
Thematic Mapper (TM)	Band 1 – Blue	0.45–0.52	30
	Band 2 – Green	0.52–0.60	30
	Band 3 – Red	0.63–0.69	30
	Band 4 – Near Infrared (NIR)	0.76–0.90	30
	Band 5 – Shortwave Infrared (SWIR) 1	1.55–1.75	30
	Band 6 – Thermal	10.40–12.50	120
	Band 7 – Shortwave Infrared (SWIR) 2	2.08–2.35	30
Landsat 8 Operational Land Imager (OLI) and Thermal Infrared Sensor (TIRS)	Band 1 – Ultra Blue (coastal/aerosol)	0.435–0.451	30
	Band 2 – Blue	0.452–0.512	30
	Band 3 – Green	0.533–0.590	30
	Band 4 – Red	0.636–0.673	30
	Band 5 – Near Infrared (NIR)	0.851–0.879	30
	Band 6 – Shortwave Infrared (SWIR) 1	1.566–1.651	30
	Band 7 – Shortwave Infrared (SWIR) 2	2.107–2.294	30
	Band 8 – Panchromatic	0.503–0.676	15
	Band 9 – Cirrus	1.363–1.384	30
	Band 10 – Thermal Infrared (TIRS) 1	10.60–11.19	100
	Band 11 – Thermal Infrared (TIRS) 2	11.50–12.51	100

Fig. 1. Features of Landsat 5 TM and Landsat 8 OLI/TIRS satellite images [28]

Temperature differences between day and night are intense and freeze-thaw cycles are effective most of the year. Therefore, it is of critical importance in terms of snow-cover monitoring and management. The wide coverage provided by remote sensing data offers significant advantages in terms of monitoring snow cover dynamics and producing results quickly [27]. In this study, Landsat 5 (August 1988, 2000, 2010) and Landsat 8 level 1A satellite images (August 2020) were used in the classification of snow cover and other areas. The data were downloaded from the United States Geological Survey (USGS) website freely. Fig. 1 describes the dataset in detail. The study area is divided into two main classes: snow cover and other areas. Fig. 2 shows the satellite images of the study area in RGB band combination.

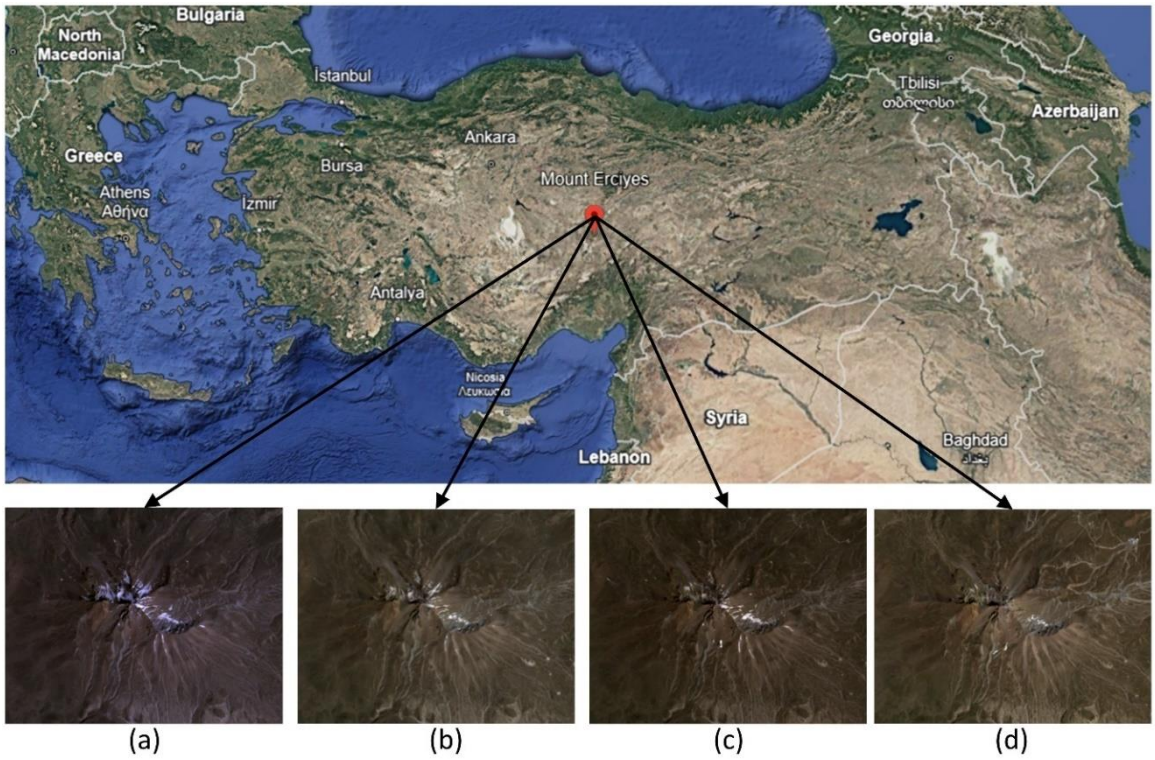

Fig. 2. Satellite images of Erciyes Mountain: (a) 1988, (b) 2000, (c) 2010, (d) 2020

3. Methodology

The classification and change detection approach used to determine snow cover changes with the aid of unsupervised classification methods is presented in Fig. 3. Firstly, Landsat satellite images were subjected to image preprocessing (geometric, radiometric, and atmospheric correction) processes according to the study flowchart. Then, atmospherically corrected Landsat satellite images were used to obtain snow cover areas using three different unsupervised classification methods (R/SWIR, NIR/SWIR, and NDSI). Finally, comparative analysis of the classification methods was performed and the snow cover area change was evaluated.

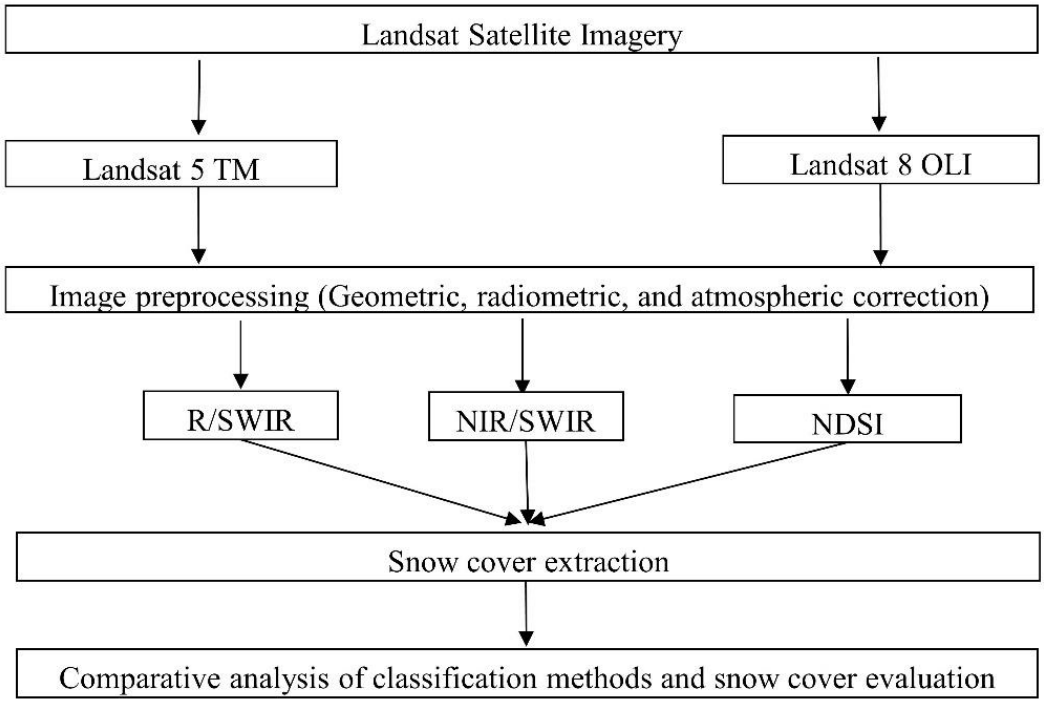

Fig. 3. Flowchart of study

3.1. Image Preprocessing

Initially, a study area was created from the peak to the mountain's slopes. The study area boundaries were used for all satellite data. Geometric correction, one of the image preprocessing stages, aims to align and rectify the image data to represent the geographic features and spatial relationships accurately. This process is carried out using ground control points (GCPs), which are known coordinates located at the same geographic position in both the reference image and the image to be transformed. These GCPs are evenly distributed across the image [29]. The geometric correction process resulted in a root mean square error (RMSE) value of 0.1 pixels in this study.

In change detection studies, it is significant to prefer satellite images with identical spatial and radiometric resolution to reduce errors caused by factors such as variations in sun angle, seasonal differences, or the satellite's position when using images from different years. Therefore, radiometric correction should be performed. This was achieved by transforming pixel brightness values of satellite images to spectral radiance values. Later, Spectral radiance values were processed using the FLAASH atmospheric correction in ENVI 5.3 software. This approach was implemented to effectively eradicate influences from reflected energy.

In this study, three different unsupervised image classification methods (R/SWIR, NIR/SWIR, and NDSI) were used to investigate which method would determine the snow cover most accurately.

3.2. Red/Shortwave Infrared Band Ratio

The Red / Shortwave infrared (R/SWIR) band ratio is an effective unsupervised classification method used to determine snow cover. This ratio is calculated by comparing the reflectance values of the red (R) and shortwave infrared (SWIR) bands. The formula is as Equation 1 follows [30]:

$$Band\ Ratio_1 = \frac{R}{SWIR} \tag{1}$$

The reflectance values in Landsat 5 TM bands 3 and 4 are denoted as R and SWIR. In Landsat 8 OLI, Band 4 and 5 correspond to R and SWIR because of the spectral bandwidth match. Snow shows high reflectance in the R band and low reflectance in the short-wave infrared. Therefore, this ratio is an effective tool for determining snow cover [30].

3.3. Near Infrared/Shortwave Infrared band ratio

The Near infrared / Shortwave infrared (NIR/SWIR) band ratio is another effective unsupervised classification method for determining snow cover. This ratio is calculated by comparing the reflectance values of the near-infrared (NIR) and short-wave infrared (SWIR) bands. The formula is as Equation 2 follows [30]:

$$Band\ Ratio_2 = \frac{NIR}{SWIR} \tag{2}$$

NIR and SWIR denote the reflectance values in Landsat 5 TM bands 4 and 5. Because of the spectral bandwidth match, the values for bands 5 and 6 correspond to NIR and SWIR in Landsat 8 OLI. Snow shows high reflectance in the NIR band and low reflectance in the SWIR band. This feature helps to distinguish snow cover from other surface types. Wang, Wang [16] used this method for snow cover mapping in dense coniferous forests. They emphasized that this method is one of the most effective methods used in snow cover mapping studies.

3.4. Normalized Difference Snow Index

Normalized Difference Snow Index (NDSI) is one of the important unsupervised classification methods used to determine snow cover areas thanks to the wide-area observations provided by remote sensing data. NDSI is calculated with the reflectance values of the green band (G) and SWIR bands. The formula is as Equation 3 follows [31]:

$$NDSI = \frac{(G - SWIR)}{(G + SWIR)} \tag{3}$$

The reflectance values in Landsat 5 TM bands 2 and 5 are denoted as G and SWIR. In Landsat 8 OLI, Bands 3 and 6 correspond to G and SWIR due to spectral bandwidth matching. NDSI values of 0.4 and above generally indicate the presence of snow cover [31]. Knowing the threshold value accelerates the snow cover monitoring and mapping processes, allowing researchers to obtain rapid results.

3.5. Snow Cover Extraction

The effectiveness of unsupervised classification methods (R/SWIR, NIR/SWIR, and NDSI) in snow cover extraction was analyzed in the current study. It was necessary to subject the classified images to a thresholding process to obtain the desired snow-covered areas using the classification methods employed in this study. Initially, Otsu's binary thresholding method [32, 33] was utilized to determine the threshold value. However, when the threshold values obtained using Otsu's method were applied, it was observed that the snow-covered areas could not be accurately detected in all three methods. Racoviteanu, Arnaud [34] suggested that the threshold value for classified images can be determined through careful visual inspection. Therefore, threshold values were determined using image histograms after visually analyzing the R/SWIR and NIR/SWIR classification images. For the NDSI classification images, the threshold value ≥ 0.4 was used as determined in previous studies [31, 35, 36]. Thus, places equal to or greater than the specified threshold value (NDSI ≥ 0.4) were determined as snow areas.

3.6. Performance Metrics

A confusion matrix is utilized to assess the performance of a classification model by comparing the predicted classifications to the actual classifications. It provides a wide summary of the classification results, allowing for the calculation of various performance metrics, including True Positives (TP), True Negatives (TN), False Positives (FP), and False Negatives (FN), as shown in Table 1 [37].

Table 1. Confusion matrix

Predicted Model	Ground Truth	
	Correct	Incorrect
Correct	TP	FP
Incorrect	FN	TN

In snow cover classification, TP refers to correctly identified snow-covered pixels, while TN denotes correctly identified non-snow-covered pixels. Conversely, FP represents non-snow-covered pixels incorrectly classified as snow-covered, and FN signifies snow-covered pixels mistakenly classified as non-snow-covered.

Performance metrics such as accuracy and Kappa statistic value can be obtained using confusion matrix parameters [38]. Accuracy is calculated as the proportion of the sum of true positive and true negative pixels to the total number of pixels within the images, representing the extent of correct classification. The Kappa statistic is employed to quantify the degree of concurrence between a classified image and reference data, serving as a valuable metric to assess the accuracy and consistency of the classification outcomes. The performance metrics' formulas are shown in Equation 4-7 [39].

$$Accuracy = \frac{TP + TN}{TP + TN + FP + FN} \tag{4}$$

$$P_O = \frac{TP + TN}{TP + TN + FP + FN} \tag{5}$$

$$P_E = \frac{(TP + FP)(TP + FN) + (TN + FP)(TN + FN)}{(TP + TN + FP + FN)^2} \tag{6}$$

$$Kappa = \frac{P_O - P_E}{1 - P_E} \tag{7}$$

Where P_O is the observed agreement, and P_E is the expected agreement by chance.

4. Results and Discussion

In the study, three unsupervised classification methods (R/SWIR, NIR/SWIR, and NDSI) were compared using ENVI 5.3 software to extract snow cover on Erciyes Mountain. Snow cover images derived from R/SWIR, NIR/SWIR, and NDSI are shown in Fig. 4.

A confusion matrix was used to evaluate the accuracy of the classified maps. 50 ground control points covering the study area were randomly generated using ArcGIS 10.8 software. The determination of these points as snow or other areas was determined with the help of Google Earth images. The accuracy and Kappa coefficient metrics were calculated to evaluate the performance of each classification method on Landsat satellite images of different years. Classification accuracies obtained by R/SWIR, NIR/SWIR, and NDSI are shown in Table 2.

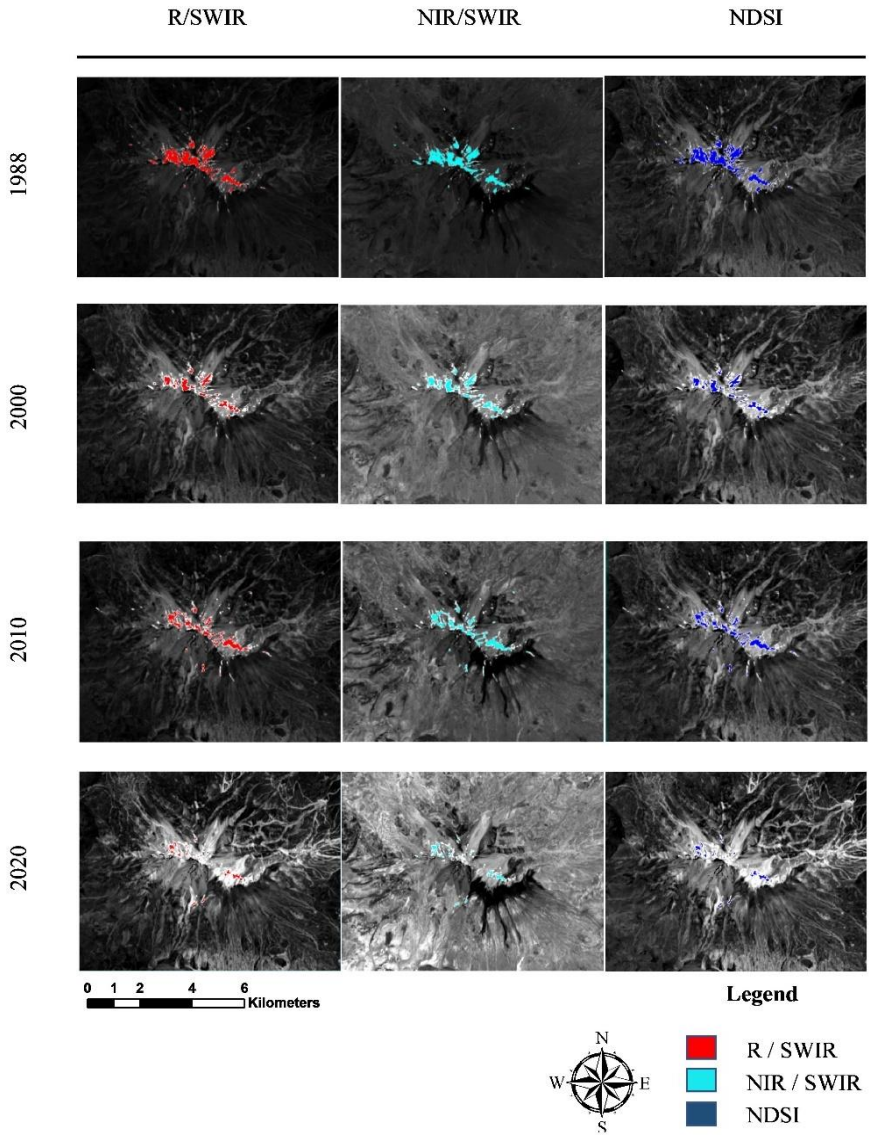

Fig. 4. Snow cover images derived from R/SWIR, NIR/SWIR, and NDSI

Table 2. Classification accuracies obtained by R/SWIR, NIR/SWIR, and NDSI

Method	R/SWIR		NIR/SWIR		NDSI	
Year	Accuracy	Kappa	Accuracy	Kappa	Accuracy	Kappa
1988	96%	86%	98%	93%	96%	86%
2000	94%	88%	90%	80%	96%	92%
2010	92%	84%	92%	84%	96%	92%
2020	92%	84%	96%	92%	98%	96%

The results reveal that the classification accuracies are generally high across the methods, with slight variations by year. For 1988, the highest accuracy (98%) and Kappa value (93%) were achieved with the NIR/SWIR method, while R/SWIR and NDSI methods showed slightly lower performance, each with 96% accuracy and an 86% Kappa value. In 2000, the NDSI method showed the best results, with 96% accuracy and 92% Kappa. The NIR/SWIR method, however, lagged behind with a 90% accuracy and 80% Kappa value. The R/SWIR method performed moderately well in 2000, achieving a 94% accuracy and an 88% Kappa. In 2010, the NDSI method continued to demonstrate superior performance,

with an accuracy of 96% and a Kappa value of 92%. Both the R/SWIR and NIR/SWIR methods achieved similar results for this year, each reaching 92% accuracy and an 84% Kappa value. Finally, for 2020, the NDSI method again yielded the highest accuracy (98%) and Kappa coefficient (96%). The NIR/SWIR method also performed well with 96% accuracy and a 92% Kappa value, while the R/SWIR method fell slightly behind, achieving 92% accuracy and an 84% Kappa value. Overall, the NDSI method consistently delivered the highest accuracy and Kappa values across different years, suggesting that it may offer more robust classification accuracy over time compared to R/SWIR and NIR/SWIR.

Table 3. Snow cover areas

Year	R/SWIR (Km^2)	NIR/SWIR (Km^2)	NDSI (Km^2)	Mean (Km^2)
1988	0.968	0.979	0.965	0.971
2000	0.414	0.437	0.404	0.418
2010	0.522	0.533	0.514	0.523
2020	0.128	0.133	0.127	0.129

An objective assessment was conducted by analyzing satellite images to account for snow cover changes from 1988-2020. Post classification comparison method was used to determine the snow cover change of the last 32 years in the study. The snow cover areas and change rates are reported in Tables 3 and 4 respectively.

Table 4. Snow cover changes according to the periods

Periods	R/SWIR Area (Km^2)	Rate (Km^2/ year)	NIR/SWIR Area (Km^2)	Rate (Km^2/ year)	NDSI Area (Km^2)	Rate (Km^2/ year)	Mean Area (Km^2)	Rate (Km^2/ year)
1988-2000	-0.55	-0.05	-0.54	-0.05	-0.56	-0.05	-0.55	0.05
1988-2010	-0.45	-0.02	-0.45	-0.02	-0.45	-0.02	-0.45	0.02
1988-2020	-0.84	-0.03	-0.85	-0.03	-0.84	-0.03	-0.84	0.03
2000-2010	0.11	0.01	0.10	0.01	0.11	0.01	0.11	0.01
2000-2020	-0.29	-0.01	-0.30	-0.01	-0.28	-0.01	-0.29	0.01
2010-2020	-0.39	-0.04	-0.40	-0.04	-0.39	-0.04	-0.39	0.04

Since the area values were close to each other, area evaluations were made by considering the average results obtained from the three methods. Table 3 shows that the highest snow covers mean value of almost 0.971 km^2 was detected in 1988 followed by the highest second value observed in 2010 with 0.523 km^2. The lowest snow cover mean value of 0.129 km^2 was observed in 2020. The lowest second value was observed in 2000 with 0.418 km^2.

In this study, the change detection approach was based on post-classification comparison [40, 41]. This method involves comparing classified images with each other to identify changes. The snow cover changes that occurred during the 32 years from 1988 to 2020 are seen in Table 4. Negative values show the total and average annual decrease in the amount of snow cover between certain periods, while positive values show the increment. According to the areas achieved from the average of results belonging to the three methods, the study showed that approximately 0.84 km^2 and 87 percent of the snow cover area had melted over the past three decades. The highest amount of snow melt was observed respectively in the periods of 1988-2000 and 2010-2020 with 0.55 km^2 and 0.39 km^2. However, there had been an increment in the snow cover area in the period of 2000-2010. This situation should be investigated further. The snow cover trend of about the past three decades can be seen in Fig. 6.

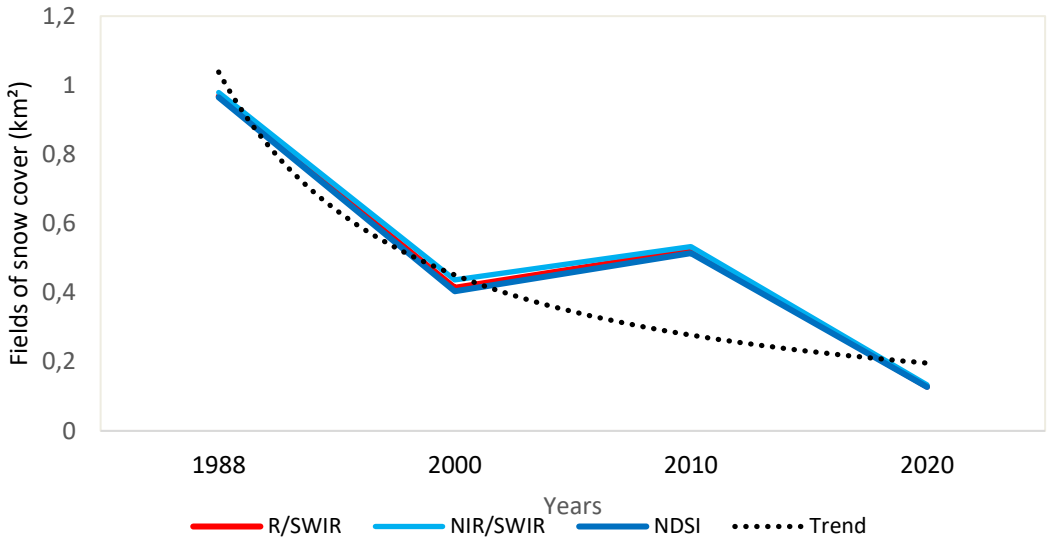

Fig. 6. Snow cover trend during the period 1988-2020

Fig. 6 indicates a significant decrease in snow cover areas between 1988 and 2020. The overall trend of snow cover change shows a decline during this period. It is investigated that the climatic conditions during the selected years to determine whether a dry climate may be responsible for the observed differences. The average temperatures and precipitations of each month over the last three decades can be seen in Fig. 7.

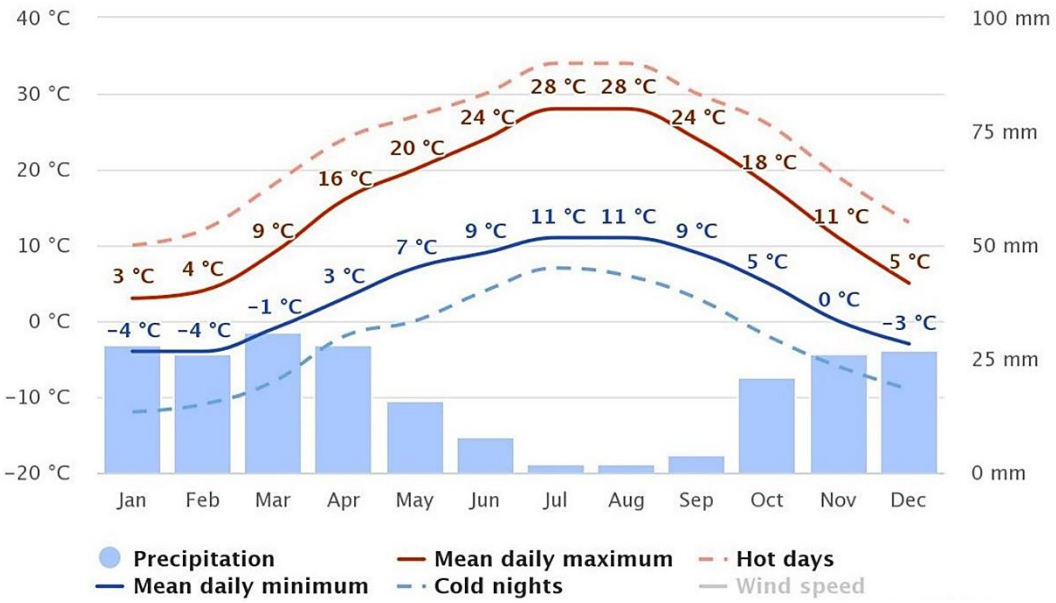

Fig. 7. Average temperatures and precipitations for Erciyes Mountain over the last three decades

As can be seen in Fig. 7, the "mean daily maximum" (represented by the solid red line) demonstrates the highest temperature recorded on an average day for each month on Erciyes Mountain. Likewise, the "mean daily minimum" (represented by the solid blue line) demonstrates the average lowest temperature recorded. The dashed red and blue lines correspond to the hottest day and coldest night, respectively, showcasing the monthly averages over the past three decades. The average temperatures on Erciyes Mountain have mostly been above 0 degrees Celsius (C°) and the precipitations below 30 mm. It is known

that high temperatures affect snowfall negatively. These data show us that global warming-based dry climate leads to a decrease in snow-covered areas in Erciyes mountain.

5. Conclusion

This study examined snow cover changes on Erciyes Mountain from 1988 to 2020, highlighting the importance of snow as crucial indicator of climate change. Changes in snow cover within mountainous regions are known to affect the continuity and sustainability of water resources significantly. By analyzing satellite imagery from different years, the study evaluated temporal trends and considered the links between these changes and the impacts of global warming. This research underscores the importance of conducting similar analyses across wider geographic areas to better understand regional trends.

The study compared the ratio-based R/SWIR and NIR/SWIR methods with the Normalized Difference Snow Index (NDSI) to determine the most effective classification method for snow cover detection. The results indicate that the NDSI method provides higher accuracy and Kappa coefficient than the other methods, establishing it as the most suitable classification approach for snow-covered mountainous areas. This suggests that the NDSI has a lower margin of error, yielding more reliable results in snow classification.

The findings show that the average snow cover area decreased from 0.971 km^2 in 1988 to 0.129 km^2 in 2020, representing an approximate 87% reduction. The most pronounced decline was observed during the periods of 1988-2000 and 2010-2020, linked to temperature increases and reduced precipitation due to climate change. However, a partial increase in snow cover was observed between 2000-2010, indicating that the complex effects of climate variations require further investigation. These findings highlight that snow cover trends offer significant insights into understanding the effects of global warming.

The study emphasizes the importance of accurate snow cover classification in mountainous regions, contributing valuable insights to future research. Improving classification accuracy enables more precise analysis of regional snow cover changes, which can inform local climate adaptation strategies. Therefore, further analysis of alternative classification methods for snow cover detection will be essential in advancing research on climate change impacts.

References

[1] Cho E, Vuyovich CM, Kumar SV, Wrzesien ML, Kim RS, Jacobs JM. Precipitation biases and snow physics limitations drive the uncertainties in macroscale modeled snow water equivalent. Hydrology and Earth System Sciences. 2022;26(22):5721-35. https://doi.org/10.5194/hess-26-5721-2022

[2] Liu Z, Wang T, Han J, Yang W, Yang H. Decreases in mean annual streamflow and interannual streamflow variability across snow-affected catchments under a warming climate. Geophysical Research Letters. 2022;49(3):e2021GL097442. https://doi.org/10.1029/2021GL097442

[3] Yu H, Zhang X, Liang T, Xie H, Wang X, Feng Q, et al. A New Approach of Dynamic Monitoring of 5-day Snow Cover Extent and Snow Depth Based on MODIS and AMSR-E Data From Northern Xinjiang Region. Hydrological Processes. 2012;26(20):3052-61. https://doi.org/10.1002/hyp.8253

[4] Ma Y, Zhang Y. Improved on Snow Cover Extraction in Mountainous Areas Based on Multi-Factor Ndsi Dynamic Threshold. The International Archives of the Photogrammetry Remote Sensing and Spatial Information Sciences. 2022;XLIII-B3-2022:771-8. https://doi.org/10.5194/isprs-archives-XLIII-B3-2022-771-2022

[5] Atasever Ü, Kesikoğlu M, Özkan C. EvaMapper: a novel MATLAB toolbox for evapotranspiration mapping. The International Archives of the Photogrammetry, Remote Sensing and Spatial Information Sciences. 2013;40:23-6. https://doi.org/10.5194/isprsarchives-XL-7-W2-23-2013
[6] Kesikoglu MH, Cicekli SY, Kaynak T, Ozkan C, editors. The determination of coastline changes using artificial neural networks in Yamula Dam Lake, Turkey. 2017 8th International Conference on Information Technology (ICIT); 2017 17-18 May 2017. https://doi.org/10.1109/ICITECH.2017.8079936
[7] Kesikoglu MH, Atasever UH, Ozkan C, Besdok E. THE USAGE OF RUSBOOST BOOSTING METHOD FOR CLASSIFICATION OF IMPERVIOUS SURFACES. Int Arch Photogramm Remote Sens Spatial Inf Sci. 2016;XLI-B7:981-5. https://doi.org/10.5194/isprs-archives-XLI-B7-981-2016
[8] Kesikoglu MH. Evaluating spatial resolution enhancement on impervious surface detection using support vector machine. Research & Design. 2024;1(1):33-42. https://doi.org/10.17515/rede2024-003bu1111rs
[9] Jin H, chen x. Spatio-Temporal Changes of Snow Cover and Its Relationship With Meteorological Factors on the Qinghai-Tibet Plateau, China. 2021. https://doi.org/10.21203/rs.3.rs-453378/v1
[10]Xi N, Mei G. Avalanche Susceptibility Mapping by Investigating Spatiotemporal Characteristics of Snow Cover Based on Remote Sensing Imagery Along the Pemo Highway-A Critical Transportation Road in Tibet, China. Water. 2023;15(15):2743. https://doi.org/10.3390/w15152743
[11]Largeron C, Dumont M, Morin S, Boone A, Lafaysse M, Metref S, et al. Toward Snow Cover Estimation in Mountainous Areas Using Modern Data Assimilation Methods: A Review. Frontiers in Earth Science. 2020;8. https://doi.org/10.3389/feart.2020.00325
[12]Girotto M, Musselman KN, Essery R. Data Assimilation Improves Estimates of Climate-Sensitive Seasonal Snow. Current Climate Change Reports. 2020;6(3):81-94. https://doi.org/10.1007/s40641-020-00159-7
[13]Gafurov A, Vorogushyn S, Farinotti D, Duethmann D, Merkushkin A, Merz B. Snow-Cover Reconstruction Methodology for Mountainous Regions Based on Historic in Situ Observations and Recent Remote Sensing Data. The Cryosphere. 2015;9(2):451-63. https://doi.org/10.5194/tc-9-451-2015
[14]Ambinakudige S, Inamdar P, Lotfata A. A Spectral Analysis of Snow in Mt. Rainier. Journal of Geography and Geology. 2018;10(3):20. https://doi.org/10.5539/jgg.v10n3p20
[15]Butt MJ. Exploitation of Landsat Data for Snow Zonation Mapping in the Hindukush, Karakoram and Himalaya (HKH) Region of Pakistan. Hydrological Sciences Journal. 2013;58(5):1088-96. https://doi.org/10.1080/02626667.2013.799774
[16]Wang X, Wang J, Jiang Z, Li H, Hao X. An Effective Method for Snow-Cover Mapping of Dense Coniferous Forests in the Upper Heihe River Basin Using Landsat Operational Land Imager Data. Remote Sensing. 2015;7(12):17246-57. https://doi.org/10.3390/rs71215882
[17]Zhang M, Wang X, Shi C, Yan D. Automated Glacier Extraction Index by Optimization of Red/Swir and NIR /SWIR Ratio Index for Glacier Mapping Using Landsat Imagery. Water. 2019;11(6):1223. https://doi.org/10.3390/w11061223
[18]Andreadis KM, Lettenmaier DP. Assimilating Remotely Sensed Snow Observations Into a Macroscale Hydrology Model. Advances in Water Resources. 2006;29(6):872-86. https://doi.org/10.1016/j.advwatres.2005.08.004
[19]Sibandze P, Mhangara P, Odindi J, Kganyago M. A Comparison of Normalised Difference Snow Index (NDSI) and Normalised Difference Principal Component Snow Index (NDPCSI) Techniques in Distinguishing Snow From Related Land Cover Types. South African Journal of Geomatics. 2014;3(2):197. https://doi.org/10.4314/sajg.v3i2.6
[20]Kuter S, Akyürek Z, Weber GW. Estimation of Subpixel Snow-Covered Area by Nonparametric Regression Splines. The International Archives of the Photogrammetry Remote Sensing and Spatial Information Sciences. 2016;XLII-2/W1:31-6. https://doi.org/10.5194/isprs-archives-XLII-2-W1-31-2016
[21]Liu C, Huang X, Li X, Liang T. MODIS Fractional Snow Cover Mapping Using Machine Learning Technology in a Mountainous Area. Remote Sensing. 2020. https://doi.org/10.3390/rs12060962

[22]Han T, Wang D, Jiang Y, Wang X. The Stepwise Discriminant Algorithm for Snow Cover Mapping Based on FY-3/MERSI Data. 2013. https://doi.org/10.1117/12.2031490
[23]Kurter A, Sungur K. Glaciers of Middle East and Africa-Glaciers of Turkey. Satellite image atlas of the world USGS professional paper. 1991;1386:1-30. https://doi.org/10.3133/pp1386G
[24]Sarıkaya M, Çiner A, Zreda M. Late Quaternary glacial deposits of the Erciyes Volcano. Yerbilimleri. 2003;27:59-74.
[25]Yavasli DD, Tucker CJ, Melocik KA. Change in the glacier extent in Turkey during the Landsat Era. Remote Sens Environ. 2015;163:32-41. https://doi.org/10.1016/j.rse.2015.03.002
[26]Aydar E, Şen E, Sarıkaya MA, Kuzucuoğlu C. In the Footsteps of Strabon: Mount Erciyes Volcano-The Roof of Central Anatolia and Sultansazliği Basin. Landscapes and Landforms of Turkey: Springer; 2019. p. 565-76. https://doi.org/10.1007/978-3-030-03515-0_33
[27]Yu F, Wang P, Liu L, Li H, Zhang Z. The Variability of Snow Cover and Its Contribution to Water Resources in the Chinese Altai Mountains From 2000 to 2022. Remote Sensing. 2023;15(24):5765. https://doi.org/10.3390/rs15245765
[28]Afrasinei GM, Melis MT, Arras C, Pistis M, Buttau C, Ghiglieri G. Spatiotemporal and spectral analysis of sand encroachment dynamics in southern Tunisia. European Journal of Remote Sensing. 2018;51(1):352-74. https://doi.org/10.1080/22797254.2018.1439343
[29]Dave CP, Joshi R, Srivastava S. A survey on geometric correction of satellite imagery. International Journal of Computer Applications. 2015;116(12). https://doi.org/10.5120/20389-2655
[30]Pellikka P, Rees WG. Remote sensing of glaciers: techniques for topographic, spatial and thematic mapping of glaciers: CRC press; 2009. https://doi.org/10.1201/b10155
[31]Butt MJ. Characteristics of Snow Cover in the Hindukush, Karakoram and Himalaya Region Using Landsat Satellite Data. Hydrological Processes. 2012;26(24):3689-98. https://doi.org/10.1002/hyp.8375
[32]Otsu N. A threshold selection method from gray-level histograms. IEEE transactions on systems, man, and cybernetics. 1979;9(1):62-6. https://doi.org/10.1109/TSMC.1979.4310076
[33]Kesikoglu MH, Ozkan C, Kaynak T. The impact of impervious surface, vegetation, and soil areas on land surface temperatures in a semi-arid region using Landsat satellite images enriched with Ndaisi method data. Environmental Monitoring and Assessment. 2021;193(3):143. https://doi.org/10.1007/s10661-021-08916-3
[34]Racoviteanu AE, Arnaud Y, Williams MW, Ordonez J. Decadal changes in glacier parameters in the Cordillera Blanca, Peru, derived from remote sensing. J Glaciol. 2008;54(186):499-510. https://doi.org/10.3189/002214308785836922
[35]Gaur MK, Goyal R, Saha D, Singh N, Shekhar S, Kumar A, et al. The Estimation of Snow Cover Distribution Using Satellite Data in the Cold Arid Leh Region Of Indian Himalaya. Polish Journal of Environmental Studies. 2021;31(1):63-73. https://doi.org/10.15244/pjoes/135606
[36]Hall DK, Benson CS, Field WO. Changes of Glaciers in Glacier Bay, Alaska, Using Ground and Satellite Measurements. Physical Geography. 1995;16(1):27-41. https://doi.org/10.1080/02723646.1995.10642541
[37]Günen MA. Fast building detection using new feature sets derived from a very high-resolution image, digital elevation and surface model. Int J Remote Sens. 2024;45(5):1477-97. https://doi.org/10.1080/01431161.2024.2313991
[38]Stehman S. Estimating the kappa coefficient and its variance under stratified random sampling. Photogrammetric engineering and remote sensing. 1996;62(4):401-7.
[39]Revuelto J, Alonso-González E, Gascoin S, Rodríguez-López G, López-Moreno JI. Spatial Downscaling of MODIS Snow Cover Observations Using Sentinel-2 Snow Products. Remote Sensing. 2021;13(22):4513. https://doi.org/10.3390/rs13224513
[40]Kesikoğlu MH, Cicekli SY, Kaynak T. The identification of seasonal coastline changes from landsat 8 satellite data using artificial neural networks and k-nearest neighbor. Turkish Journal of Engineering. 2020;4(1):47-56. https://doi.org/10.31127/tuje.599359
[41]Kesikoğlu MH, Kaynak T. Tracking seasonal coastal dynamics of Ağyatan wetland using object-based Classification and Regression Tree. Niğde Ömer Halisdemir Üniversitesi Mühendislik Bilimleri Dergisi. 2025;14(1):308-17. https://doi.org/10.28948/ngumuh.1559034